Anal Bioanal Chem (2010) 397:2967–2976
DOI 10.1007/s00216-010-3876-4

ORIGINAL PAPER

On-chip photoactivation of heterologously expressed rhodopsin allows kinetic analysis of G-protein signaling by surface plasmon resonance spectroscopy

Konstantin E. Komolov · Mònica Aguilà · Darwin Toledo · Joan Manyosa · Pere Garriga · Karl-Wilhelm Koch

Received: 17 March 2010 / Revised: 7 May 2010 / Accepted: 24 May 2010 / Published online: 11 June 2010

Abstract Surface plasmon resonance spectroscopy allows the study of protein interaction dynamics in real-time. Application of this technique to G-protein coupled receptors, the largest family of receptors involved in signal transduction, has been complicated by their low level of expression and the critical dependence of their native conformation on the hydrophobic transmembrane lipid environment. Here, we investigate and compare three different strategies to immobilize rhodopsin, a prototypical G-protein coupled receptor on a sensor chip surface using antibodies and a lectin for receptor capturing. By further probing of different experimental conditions (pH, detergent type) we identified the optimal factors to maintain rhodopsin in a functional conformation and extended this approach to recombinant rhodopsin that was heterologously expressed in COS cells. Functional operation of rhodopsin on the sensor chip surface was proven by its activation and subsequent light-stimulated G-protein coupling. The influence of these experimental parameters on the association and dissociation kinetics of G-protein receptor coupling was determined. Thereby, we found that the kinetics of G_t interaction were not changed by the strategy of immobilization or the type of detergent. Regeneration of opsin directly on a chip allowed recycling of the immobilized native and recombinant receptor. Thus, the approach provides an experimental framework for choosing the most suitable conditions for the solubilization, immobilization, and for functional tests of rhodopsin on a biosensor surface.

Keywords Surface plasmon resonance · G-protein coupled receptor · Rhodopsin · Signal transduction

K. E. Komolov · K.-W. Koch (✉)
Biochemistry group, Faculty V, IBU, University of Oldenburg,
26111 Oldenburg, Germany
karl.w.koch@uni-oldenburg.de

M. Aguilà · D. Toledo · P. Garriga (✉)
Departament d'Enginyeria Química,
Centre de Biotecnologia Molecular,
Universitat Politècnica de Catalunya,
Colom 1,
08222 Terrassa, Spain
pere.garriga@upc.edu

J. Manyosa
Universitat Autònoma de Barcelona,
Departament de Bioquímica i de Biologia Molecular,
Unitat de Biofisica, and Centre d'Estudis en Biofísica,
08193 Bellaterra, Spain

Introduction

Heptahelical transmembrane (7TM) receptors, synonymously named G-protein-coupled receptors (GPCRs) are signaling molecules involved in a wide variety of physiological processes, ranging from neurotransmission to sensory detection. The most widely studied of these receptors are the visual pigment rhodopsin (Rho) and the β-adrenergic receptor. In recent years, the crystal structures of bovine [1] and squid Rho [2, 3], Rho photointermediates [4, 5], opsin [6] and of the β-adrenergic receptor [7] have been elucidated providing us with details on the signal transfer between the activated receptor and its G-protein. These proteins are therefore best suited as benchmarks for the study of GPCR function and corresponding signaling transduction mechanisms.

The involvement of GPCRs in central physiological processes and associated diseases make them important targets for pharmacological intervention. One of the main aspects needed to fully describe the signaling transduction mechanism mediated by GPCRs is to unravel the specific molecular features of these receptor molecules in protein–protein interaction studies including, for example, identification of interaction sites and the corresponding affinities for downstream signaling molecules. Biophysical techniques such as surface plasmon resonance (SPR) spectroscopy allow measurements of biomolecular interactions on sensor chip surfaces [8, 9]. SPR has some advantages in comparison to traditional G-protein activation methods, such as radioligand binding or fluorescence spectroscopic assays, as it enables measuring the association and dissociation rates, affinity and kinetics constants of protein–protein interactions without a label.

Nevertheless, crucial aspects for the employment of transmembrane protein in biosensor-based studies are obtaining sufficiently pure native or recombinant protein samples while retaining the intact structure and preserving the function of the receptors.

Due to the high interest in applying SPR spectroscopy to the study of receptor signaling, a variety of GPCRs have been immobilized on sensor chip surfaces in recent years for interaction studies with ligands or downstream signaling proteins. Human δ-opioid receptor [10], chemokine receptors [11], nicotinic acetylcholine receptor [12], and insulin-like growth factor-1 receptor [13], were probed in SPR studies and validated as good models for ligand screening assays and G-protein binding. Furthermore, olfactory receptor activity [14, 15] and the interaction of ligand molecules to recombinant α2-adrenergic receptor were quantitatively assessed by SPR [16].

Native Rho from bovine retina has been immobilized for SPR studies in supported lipid bilayers [17, 18], via biotin–streptavidin coupling [19] or by its interaction with the lectin ConA [20]. More recently, we have been successful in real-time monitoring transducin (G_t) interaction to native Rho, deposited on a sensor surface in a lipid bilayer free state, allowing the calculation of association-dissociation rate constants of G_t activation [21]. However, the results presented in that paper lead to several open questions related to biosensor-based studies on Rho. First, native Rho is glycosylated at two positions at the aminoterminal end and therefore can easily be captured on sensor surfaces that are coated with ConA, but heterologously expressed Rho might contain different posttranslational modifications making this strategy less suitable for immobilization of recombinant rhodopsin.

Second, detergents that are commonly used to solubilize the transmembranous Rho influence the structure and function of Rho [22], but their impact on the on-chip immobilization of Rho and on subsequent activation of signaling components like G_t has not been investigated.

Third, the application of the SPR technique to the study of non-native membrane proteins has proved specifically difficult for recombinant GPCRs, and particularly for the visual pigment Rho. So far, no SPR spectroscopy based approach has been established for studying recombinant Rho.

In the present study, we addressed the points listed above by comparing two antibody-based strategies with the ConA-based approach to immobilized Rho in a site-directed manner. Further, we tested three different detergents for theirs effects on immobilization and functional activity of Rho and developed a successful approach to analyze G-protein signaling of active recombinant Rho by SPR.

Materials and methods

Materials

CM5 sensor chips, coupling reagents and solution of SDS were from GE Healthcare Bio-Sciences AB (Uppsala, Sweden). Anti-rhodopsin monoclonal antibody rho-1D4 was from Chemicon Europe Ltd. (UK). The monoclonal antibody directed against the N-terminus of bovine Rho was kindly provided by Dr. Paul Hargrave and Dr. Clay Smith (University of Florida, USA). Concanavalin A (ConA) and 3-cholaminopropyldimethyl-ammonio-1-propane sulfonate (CHAPS) were from Serva (Heidelberg, Germany). Dodecyl-β-D-maltoside (DM), octyl-glucoside (OG), 9-*cis*-retinal and GTP were from Sigma (St. Louis, USA). All other reagents were obtained from Merck, Fluka and were at least analytical grade. Elution of the rhodopsin from rho-1D4-sepharose was carried out with a 9-mer-peptide, corresponding to the C-terminal rhodopsin sequence.

Preparation of washed ROS membranes and G_t extract

Bovine ROS were prepared from fresh bovine retinae and stored at −80 °C as described previously [23]. Hypotonically stripped disk membranes were prepared from ROS as described [24]. All steps involving non-activated Rho were performed under dim red light. Rho concentration was determined after detergent solubilization from its absorption spectrum using ε_{498}=42,000 $M^{-1}cm^{-1}$. A G_t extract was obtained as described before [25] and was stored at −80 °C until use.

Transfection of COS-1 cells and purification of recombinant rhodopsin

COS-1 cells were transfected with the wild-type (WT) opsin gene by means of a DEAE-dextran method as previously described [26]. The transfected cells from five

150-mm diameter tissue culture plates were harvested 60 h after transfection, washed with buffer A (1.8 mM KH_2PO_4, 10 mM $NaHPO_4$, 137 mM NaCl, and 2.7 KCl; pH 7.2) and resuspended in 10 mL of the same buffer. Regeneration with 9-*cis*-retinal (50 μM) was carried out in the dark with gentle stirring for 3 h at 4°C. The cells were then solubilized either with 1% DM or 50 mM CHAPS for another 1 h under the same conditions. The solubilized cells were subsequently centrifuged at 88,000×*g* for 30 min at 4°C, and the supernatant was applied to 200 μL of a rho-1D4-sepharose batch for purification. After incubation for 3 h with gentle shaking, the resin was washed five times with 1 mL of buffer A containing 0.05% DM or 5 mM CHAPS, respectively. Elution of Rho was performed with 200 μL of buffer A containing 100 μM of the Rho C-terminal 9-mer-peptide and 0.05% DM or 25 mM CHAPS, respectively.

Western blot analysis

Western blot analysis of Rho was carried out using the Rho-1D4 monoclonal antibody which recognizes the last 8 amino acid residue of the C-terminal tail of Rho as previously described [27].

SPR spectroscopy

SPR measurements were performed on a Biacore 2000 (GE Healthcare). Details of the operation principle, the immobilization procedures and of the evaluation of sensorgrams had been previously described [8, 21, 28]. The SPR running buffer was 50 mM MOPS, pH 7.5; 150 mM NaCl; 3 mM $MgSO_4$; 10 μM $CaCl_2$; 10 μM $MnCl_2$.

Immobilization of ConA, 1D4 antibody, and antibody against rhodopsin N-terminus

ConA and antibodies against the C-terminus (1D4) and N-terminus of Rho were used capturing Rho on the dextran surface of the sensor chip. Anchor proteins were immobilized by amine linkage to dextran was described in detail previously [21]. The concentration of the antibodies used for immobilization was 0.1 mg/mL.

Capture of native and recombinant rhodopsin

Dark-adapted ROS membranes were solubilized in 25 mM CHAPS (final concentration) at 4°C for 30 min (gentle shaking) in order to prepare native Rho for effective capture onto the chip surface. We also tested 1% DM or 50 mM OG to extract native Rho from ROS membranes. After detergent solubilization, insoluble material was separated from soluble Rho by centrifugation (17,000 rpm rotor S100-AT from Sorvall, 15 min at 4°C). The solubilized Rho sample was diluted five times, before injection, with 50 mM MES pH 6.0, 1 mM $CaCl_2$, 1 mM $MnCl_2$ to reach a final concentration of 0.4 mg/mL Rho (flow rate was 2 μL/min; injection volume was 50 μL). The sample of purified recombinant Rho was also diluted five times with the MES buffer at pH 5.0. The lower pH allowed a higher immobilization level of recombinant Rho. The stability of the Rho sample was checked by measuring the UV–Vis spectrum. Immediately after the end of the injection, the sensor chip surface with immobilized recombinant Rho was washed with SPR running buffer at high flow rate (30 μL/min) until a stable base line was reached (usually after 30 min). Corresponding resonance units were used for the calculation of protein densities by means of the Biacore standard relation of 1 resonance unit (RU) = 1 pg of protein/mm^2.

G_t binding to immobilized rhodopsin

Measurements of light-triggered binding of G_t to Rho was performed on a modified Biacore system using an optical fiber connected to a Diode Pumped Nd-YAG solid state laser (λ=532 nm) allowing direct activation of Rho on the surface of the sensor chip. Details of the operations have been described previously [21]. Detailed care was taken to use a suitable control accounting for non-specific interactions. Briefly, G_t was injected over the Rho-coated surface and the corresponding sensorgram was first recorded in darkness. Subsequently, the same recording was performed for light-triggered binding of G_t to Rho. The sensorgrams obtained in darkness were always subtracted from the ones recorded after illumination in order to correct for non-specific interaction of G_t and the sensor chip surface.

Rate constants were calculated by nonlinear fitting of the primary sensorgram data using BIAevaluation 4.1 software. Bulk refractive index changes that originated from a change in running solution were subtracted in order to facilitate recognition of protein binding and dissociation steps. Random occurring spikes were eliminated by the BIAevaluation cut function. Exact concentration of G_t in the applied G_t extract was calculated by densitometric analysis of G_t bands in Coomassie Brilliant Blue-stained gels using known amounts of purified G_t as standards for proper calibration of G_t quantities.

Regeneration of Rho and of Rho-coated surfaces

The chip surface was regenerated after every cycle of illumination and G_t binding. Due to a limited supply of 11-*cis*-retinal, commercially available 9-*cis*-retinal (which is known to have an analogous behavior to the 11-*cis*-retinal isomer) was used to regenerate Rho. Regeneration was

performed directly on the chip surface by injecting 300 μL of a 10 μM solution of 9-*cis*-retinal (diluted from 100 mM stock solution by SPR running buffer just before injection) at a low flow rate (1 μL/min). Alternatively, the surface could be regenerated by removing Rho from the antibody surface and ConA by five consecutive injections of a 0.05% SDS solution for 1 min at a flow rate of 20 μL/min.

Results and discussion

Different approaches for receptor immobilization on a biosensor surface

Although native Rho can be effectively immobilized and studied by employing lectin ConA as an anchor protein [21], the application of the same approach using heterologously expressed Rho was unexpectedly difficult. The heterogeneous glycosylation of Rho expressed in mammalian cell cultures hampered the immobilization of recombinant Rho onto the sensor chip via ConA approach. To overcome this difficulty, we tested other approaches for specific immobilization of native and recombinant Rho that would preserve the functional properties of the receptor and would allow their light-triggered binding to the G-protein G_t. An attractive alternative for attachment of Rho to the biosensor surface was to use specific antibodies that would provide unambiguous binding sites for Rho. For that purpose, we tested the capturing properties of two different antibodies directed against the N- and C-terminus of Rho respectively, and compared it with ConA-based experiments. The proteins recognize specific regions of Rho leading to its uniform orientation on the sensor surface. ConA and the antibody directed against the N-terminus capture Rho in a way that the C-terminus is pointing to the bulk medium (Fig. 1). The 1D4 antibody is directed against the C-terminus of Rho and would result in a contrary orientation of the Rho molecule on the surface, with the N-terminus extending to the bulk medium. Antibodies and ConA were immobilized at similar densities on the sensor chip (Table 1 and Fig. 2a). Prepared surfaces were used to capture native dark-adapted Rho, extracted from ROS membranes using the CHAPS detergent. Although the immobilization was successful in every case, solubilized Rho was retained at different densities on the sensor chip surface (Fig. 2a) yielding an apparent higher density with the 1D4-coated surface than with the other surfaces (Table 1). The overlay shown in Fig. 2 is representative of at least three independent experiments, in which we always observed differences in immobilization yields. Different levels of Rho immobilization and also different ratios of Rho per anchoring molecule (Table 1) might arise from the different geometric features of anchoring Rho. Immobilization of Rho by the 1D4-antibody occurs via the C-terminus, whereas the other two surfaces (ConA and antibody against the N-terminus) capture Rho at the opposite site. Binding via the C-terminus might allow binding of dimeric or oligomeric Rho that is known to be present in detergent mixtures [22], but binding to the N-terminus might capture Rho in a monomeric state.

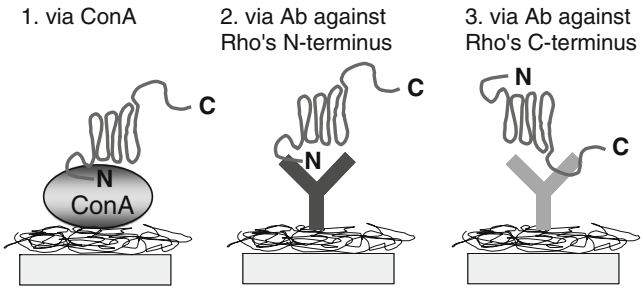

Fig. 1 Strategies used for capturing Rho on a biosensor surface. ConA and the antibody against the N-terminus bind Rho at its N-terminal site. An opposite orientation of Rho is achieved upon immobilization onto a 1D4-coated surface with the C-terminus of Rho bound to the antibody

Functional test of immobilized Rho

Although the immobilization strategies seemed suitable for an interaction analysis, a critical test to prove the function of Rho was to measure its light-triggered interaction with G_t. Therefore, G_t was injected over the surface containing immobilized dark-adapted Rho and the binding of G_t to Rho was initiated by illuminating the sensor chip surface (Fig. 2b). Interaction of G_t to Rho was detected in all cases but differed in the amount of bound G_t. Surprisingly, the binding of G_t to Rho captured on 1D4-coated surface was more effective than in cases where Rho was immobilized via its N-terminus. Not only was the total amount of bound G_t higher, but also the ratio of bound G_t to immobilized Rho was larger (Table 1). This ratio indicates the amount of functional Rho that is able to bind to G_t in relation to the total amount of receptor deposited onto the chip surface. Intuitively, one would expect to find a higher ratio of G_t bound to immobilized Rho when the C-terminus is free of an interacting partner because the Rho–G_t interaction takes place on the cytoplasmic side of the receptor where the C-terminus is located. Instead, the opposite was reproducibly found. Further, when we analyzed the association and dissociation kinetics of G_t interaction by nonlinear curve fitting using BIAevaluation 4.1, we saw no difference among the different immobilization strategies resulting in rather similar affinities of Rho–G_t interaction (Table 2). Interestingly, the K_D values were similar to the K_D value (18 nM) that was reported in a plasmon-waveguide resonance spectroscopy study on photoactivated rhodopsin in nonlamellar-forming lipids [29]. Association rate con-

Table 1 Summary of the data on the immobilization of the anchor proteins, Rho and G_t binding, presented in Fig. 2. The number of bound proteins was calculated by using the Biacore standard relation of 1 resonance unit (RU) = 1 pg of protein/mm^2

Anchor protein	Anchor protein density (10^{11} molecules)	Rho density[a] (10^{11} molecules)	Degree of anchor protein occupation (Rho/anchor protein)	G_t[c] amplitude (10^{11} molecules)	G_t/Rho
ConA (28 kDa)	1.15 (5360 RU)	0.94 (7490 RU)	0.82	0.052 (747 RU)	1/18
Ab against C-terminus (150 kDa)	0.21 (5111 RU)	1.36 (10883 RU)	3.24[b]	0.116 (1641 RU)	1/12
Ab against N-terminus (150 kDa)	0.25 (6152 RU)	0.35 (2780 RU)	0.7[b]	0.019 (267 RU)	1/18

[a] The size of a Rho micelle in CHAPS is 48.15 kDa

[b] Assuming that 1 molecule of Ab has 2 binding sites for Rho

[c] Molecular mass of G_t is 85 kDa

stants (k_a) were around 3.4×10^4 $M^{-1}s^{-1}$ and dissociation rate constants (k_d) around $4.7\times10^{-4}s^{-1}$, which indicates that in all cases G_t had similar access to the binding site in Rho. We conclude from these results that the capture of Rho via 1D4 antibody not only does not interfere with a subsequent Rho–G_t interaction but improves it. Furthermore, this orientation seems to favor G_t binding and activation processes.

A few other GPCRs including the human olfactory receptor 17–40 and the chemokine receptors [11, 14] were successfully immobilized via the C-terminus and the 17-40-receptor remained functional [14].

The rational explanation of the observed effect could be found in structural features of the receptors. The C-terminus of Rho is exposed to the cytoplasm and highly mobile and flexible [30, 31]. Moreover, the recognition site of 1D4 antibody is a small part of the C-terminus of Rho and localized at its very end (last nine C-terminal amino acids). Thus, binding of the antibody would not preclude some freedom for a wagging motion of the receptor allowing free access and efficient G_t binding. A potential explanation for the higher efficiency in the 1D4 case would be that when Rho binds to the antibody, through its epitope at the C-terminal tail, it adopts such a conformation that is able to "trap" the incoming G_t protein between the antibody and the receptor, and positioning it in a more productive way for interaction with the receptor. However, our kinetic analysis yielded similar k_a and k_d values for each Rho geometry on the chip surface. So one would expect a different set of constants, if G_t gets trapped during the binding process, which is not the case. Therefore, we think that the positive effect of the 1D4 antibody in immobilization is to keep more Rho molecules in a functional state.

Effect of the detergent type on capture and functional properties of native Rho

The important factor for functional integrity and stability of membrane proteins is the selection of an optimal appropriate detergent for solubilization. We tested and compared three detergents, which are commonly used for Rho solubilization. These are CHAPS, DM, and OG that represent different classes of detergents and maintain a relatively high thermal stability of Rho [32], but they also have different effects on the oligomer–dimer–monomer equilibrium of Rho [22]. Comparing different detergents in SPR studies will be particularly important for processing Rho mutants, which often show a decreased thermal stability. We tested the ability of these detergents to maintain native Rho in an intact, active state during extraction from membranes and immobilization on the 1D4-coated biosensor surface. The density of Rho on the surface upon immobilization was almost the same for CHAPS- and OG-solubilized Rho (5,200 and 4,900 RU, respectively), and slightly higher in the case of the DM-extracted receptor (6,700 RU; Fig. 3a). But when we applied G_t into the flow cell system to check the functional properties of Rho we observed very different amplitudes of G_t binding (Fig. 3b). G_t binding to CHAPS-solubilized Rho was 2.6- and 7.2-fold higher than OG- or DM-solubilized Rho, respectively. Kinetic evaluation resulted in similar values for k_a and k_d (Table 2) showing that the interaction with G_t occurs with similar affinities, but according to the different binding amplitudes more Rho molecules are in a functional state on the chip surface when CHAPS was employed. This clearly highlights the profound impact of the type of detergent on the functional properties of Rho when it is deposited on a biosensor.

Treatment of ROS membranes with CHAPS or DM causes extraction of different Rho association states. Whereas CHAPS-solubilized Rho was found mostly in dimeric or oligomeric forms, solubilization with DM led to extraction of mostly monomeric form of the receptor [22]. The oligomerized Rho appeared to better resemble the native state of Rho in membranes and could be therefore better suited towards G_t binding than the monomeric form. Further, the higher critical micellar concentration of CHAPS and OG corresponds with a larger amount of lipids

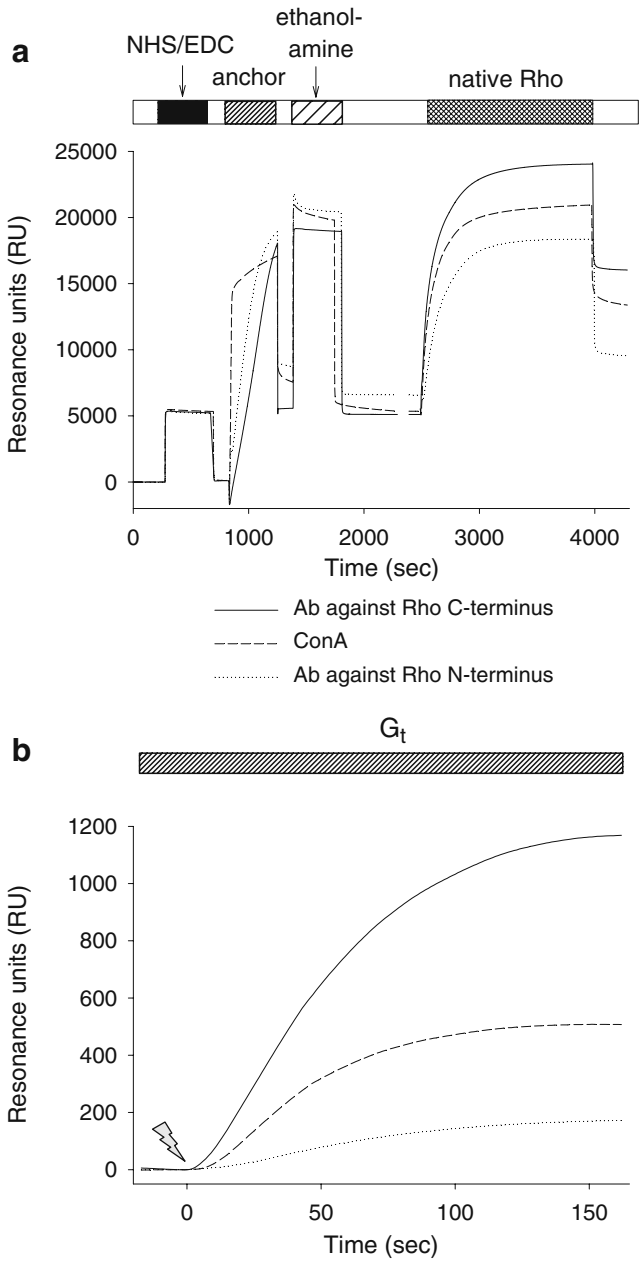

Fig. 2 Anchoring native Rho on different surfaces and subsequent G_t binding. **a** Sensorgrams of Rho immobilization as monitored by SPR spectroscopy. The bars indicate the sequential injections of the *N*-hydroxysuccinimide/carbodiimide (NHS/EDC) mixture to activate the carboxyl groups on dextran, followed by injections of the anchoring proteins. Ethanolamine was injected to inactivate unreacted surface groups. The capture of dark-adapted CHAPS-solubilized native Rho is shown with the last injections. **b** Test to prove whether Rho maintained its functional properties on the different surfaces. A G_t extract was injected over immobilized dark-adapted Rho. Specific light-induced binding of G_t was triggered by continuous laser illumination of the chip surface at t_0=0. *Line drawings of sensorgrams* are the same as used in part **a**

associated with solubilized Rho upon detergent dilution [33]. The ability of CHAPS to extract a higher amount of phospholipids may better preserve the native organization of Rho.

Influence of pH and detergent type on immobilization of recombinant Rho

SPR studies with recombinant Rho required the purification of heterologously expressed Rho from a cell suspension. Rho can be routinely expressed in COS-1 cells, regenerated with 11-*cis*-retinal (or with the 9-*cis*-retinal analog) and can be used in functional in vitro studies [34]. We employed the same procedure and purified Rho by an immunoaffinity column (1D4-sepharose). The purification step was necessary due to high non-specific precipitation of cell material on the sensor chip surface (not shown). Furthermore, it was essential for subsequent functional SPR studies (see below) that expression of Rho in COS cells was high enough and that the UV–Vis spectral characteristics of purified Rho indicated the presence of regenerated Rho and not of misfolded Rho species.

Since carboxy-dextran coated sensor chips contain a high number of negatively charged carboxy groups, any immobilization procedure has to find the right balance between repulsion and attraction by adjusting the pH of the running and immobilization buffers. Native Rho could be immobilized at different values of pH with sufficient yields to result in efficient G_t-coupling. However, we observed a strong influence of the pH on the immobilization yield of recombinant Rho. We compared the immobilization level of immunopurified recombinant Rho at pH 7, pH 6 and pH 5 (Fig. 4a). Just before injection, the pH of the Rho solution was adjusted to the needed values and then applied for immobilization on the antibody surface (1D4-coated flow cell). A reasonable immobilization level was only observed at pH 5. At pH 7 and pH 6 the capture of Rho by the 1D4 antibody was too low for performing subsequent interaction studies (we previously established with native Rho that the Rho density on a biosensor surface should be ≥500 RU in order to detect light-triggered interaction with G_t). The p*I* of rhodopsin is around 5.5–6, so pH 5 would be below the p*I* and in this situation the molecule would have a net positive charge. This favors the prebinding of Rho to the negatively charged surface (see above) and finally facilitates the immobilization to the anchor proteins.

Sufficient immobilization levels were then achieved, when purified recombinant Rho was immobilized at pH 5 using CHAPS. A comparison of sensorgrams obtained with Rho purified in CHAPS or DM is shown in Fig. 4b. Using CHAPS led to faster kinetics of receptor immobilization and finally resulted in higher immobilization level of recombinant Rho. CHAPS was also better for preserving functional stability of recombinant Rho on the sensor chip surface since we detected G_t binding only to CHAPS-extracted Rho but not to the DM-extracted protein (see also below).

Table 2 Kinetic analysis of G_t binding to Rho, immobilized on the sensor chip surface via different anchor proteins and purified with the different detergents (Figs. 2 and 3)

Concentration of G_t in G_t extract was 120 nM (see the "Materials and methods" section)

	k_a, M^{-1} s^{-1}	k_d, s^{-1}	K_D, nM
Effect of anchor protein			
ConA	$(3.6\pm0.7)\times10^4$	$(3.9\pm0.9)\times10^{-4}$	15.9±4.9
Ab against C-terminus	$(3.2\pm0.7)\times10^4$	$(4.8\pm1.1)\times10^{-4}$	20.6±8.9
Ab against N-terminus	$(3.4\pm0.9)\times10^4$	$(5.3\pm1.8)\times10^{-4}$	20.0±8.7
Effect of detergents			
CHAPS	$(3.3\pm0.6)\times10^4$	$(4.1\pm1.0)\times10^{-4}$	14.2±5.1
DM	$(4.2\pm1.2)\times10^4$	$(5.4\pm1.8)\times10^{-4}$	13.8±6.9
OG	$(2.9\pm1.1)\times10^4$	$(4.3\pm2.8)\times10^{-4}$	17.6±8.3

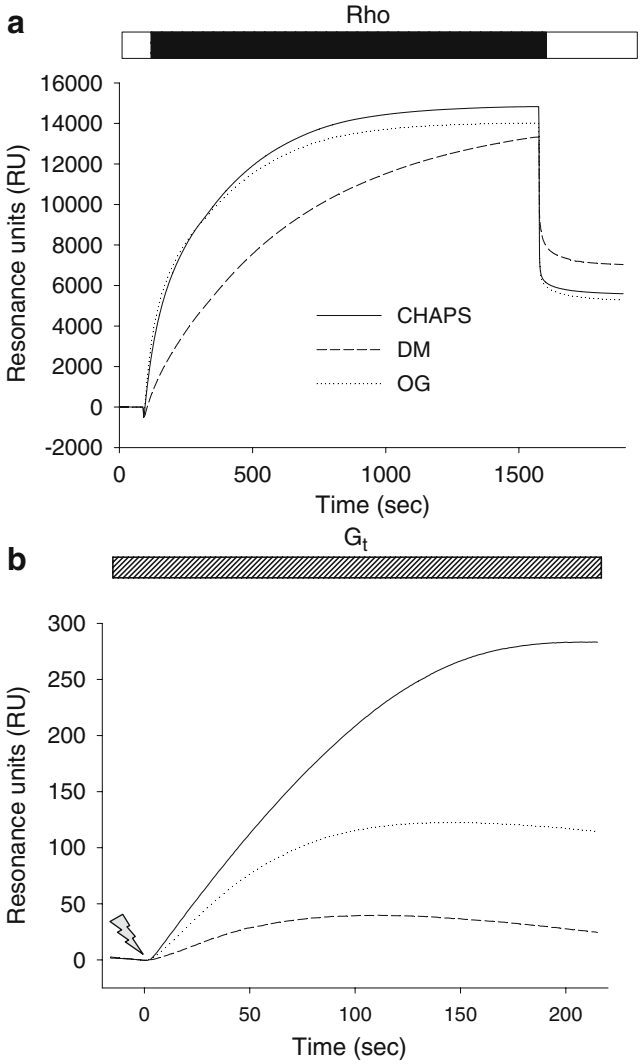

Fig. 3 Effect of detergent on immobilization and functional activity of native Rho on a biosensor surface. **a** Sensorgrams of Rho immobilization that was previously solubilized with the detergents DM, OG or CHAPS and injected over the 1D4-coated surface. **b** Functional test on light-triggered binding of G_t to immobilized Rho. Sensorgrams represent the G_t binding signal after illumination of the surface. Line drawings of sensorgrams are the same as used in part A

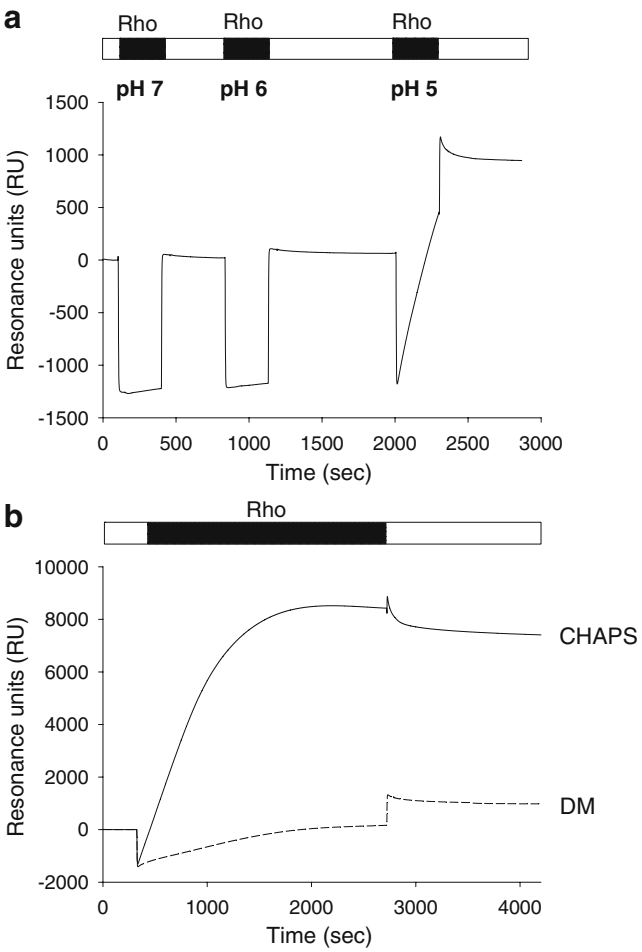

Fig. 4 Influence of pH and detergent type on the capture of recombinant Rho on the 1D4-coated surface. **a** Immobilization of purified recombinant Rho at different pH that was adjusted directly before injections. **b** DM/CHAPS effect on the capture of recombinant Rho. Recombinant Rho was purified by using either DM or CHAPS as a solubilizing agent and then immobilized on the 1D4-coated surface. The concentration of DM and CHAPS during immobilization was 0.2 and 5 mM, respectively

In situ activation of recombinant Rho on the sensor chip surface

The functional operation of recombinant Rho was proved by its light-dependent interaction with G_t. For this purpose, immobilization of dark-adapted Rho was followed by G_t injection. Illumination of the sensor chip induced an increase of the resonance signal (Fig. 5) indicating G_t binding to photoactivated Rho. A stop of G_t injection resulted in a slow dissociation of nucleotide-free G_t. Fast and complete dissociation of G_t from the surface was achieved by injection of GTP. The kinetic constant was determined from the analysis of association and dissociation phases of G_t binding by BIAevaluation 4.1 software. The calculated dissociation rate constant (k_d) was 1×10^{-4} s^{-1} and the association constant (k_a) was $1.1\times10^{4}M^{-1}s^{-1}$ which resulted in K_D=9.1 nM for the Rho–G_t interaction in the absence of GTP. Therefore, the defined affinity constant for the interaction of recombinant Rho with G_t is in good agreement with the K_D of 13.6 nM that we obtained previously by SPR measurements for native Rho [21].

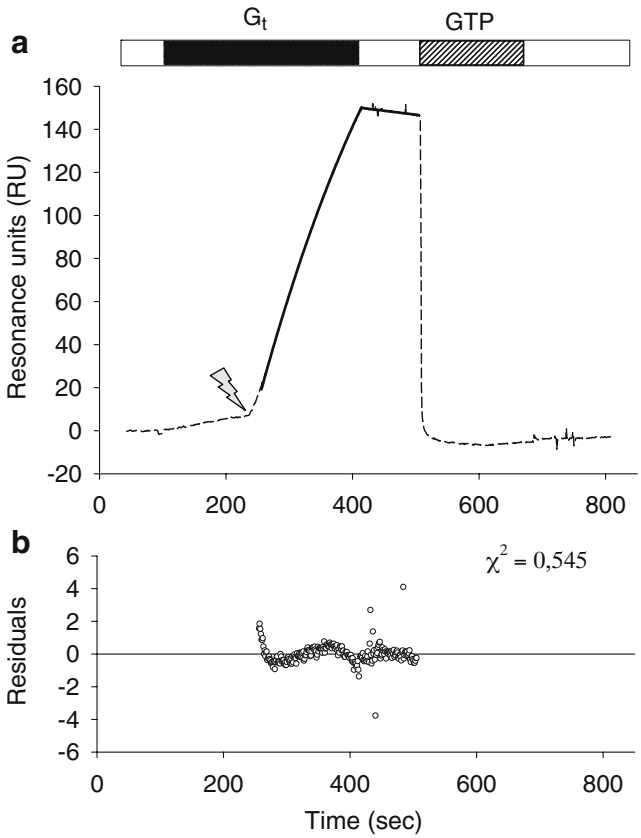

Fig. 5 Interaction of G_t with recombinant Rho monitored by SPR. Dark-adapted Rho was immobilized on the sensor chip surface via 1D4 antibody and kept in the dark. Illumination of the sensor chip surface triggered on-chip activation of Rho and led to the binding of G_t as indicated by the fast increase of resonance units. The running buffer (*open bar*) after G_t injection (*black bar*) initiated a slow dissociation of G_t from the complex with bleached Rho. Fast and complete dissociation of G_t was triggered by injection of GTP (*hatched bar*). The K_D of nucleotide-free G_t/Rho interaction was calculated from on- and off-rates of the interaction and was 9.1 nM. Corresponding fits are indicated as *bold lines*. Residuals of the fit and the value of χ^2 are shown in the *lower part of the figure*

On-chip regeneration of Rho

Recovery of Rho activity after an activation cycle is a prerequisite for an elaborate and reliable use of the receptor coated surface. Regeneration could be performed directly on the chip surface by 5 h injecting 9-*cis*-retinal into the flow cell. Upon regeneration procedure, recombinant Rho showed 80–90% of its original activity with respect to G_t binding (Fig. 6). Longer treatment did not result in higher regeneration yields, apparently due to a non-active pool of Rho molecules on the surface that was probably denatured during activation and regeneration cycles. The regeneration procedure with 9-*cis*-retinal could be repeated several times with the same Rho pool on the surface allowing repeated cycles of rhodopsin-coupled signaling.

Conclusions

The GPCR superfamily is a wide class of cell receptors that are currently being investigated as one of the main targets

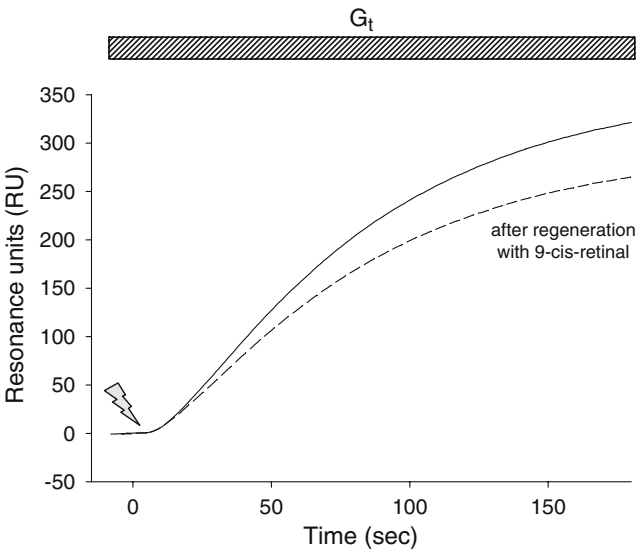

Fig. 6 Rescue of recombinant Rho functionality after on-chip regeneration with 9-*cis*-retinal. The sensorgrams represent an overlay of two plots obtained during injection of the G_t extract before and after regeneration of Rho. Recombinant Rho was immobilized on the 1D4-coated surface and applied for light-triggered G_t binding (full line). All bound G_t completely dissociated from the surface after GTP injection (not shown). Following 5 h treatment of Rho with 10 μM 9-*cis*-retinal, almost all functional activity of immobilized Rho was recovered, as indicated by a similar G_t binding signal (*dashed line*)

for new drug discovery and the development of novel therapeutic approaches. It is, thus, of great importance to find out optimal conditions for studying these receptors and the interaction features with their signaling transduction partners. By testing a number of different experimental conditions we investigated the properties of native and recombinant Rho using SPR sensor chips. We have found that recombinant Rho solubilized with CHAPS detergent and immunopurified from COS cells debris can be successfully immobilized via 1D4 monoclonal antibody as an anchoring molecule onto the sensor chip surface to further study kinetics of G-protein signaling by SPR. The 1D4 antigenic site in rhodopsin has been used as a tag in other studies in which recombinant GPCRs and other membrane proteins were affinity-purified [35]. By this approach, 1D4-tagged receptors could also be applied in future SPR studies. Thus, our approach can have general implications for SPR studies of GPCRs and opens the way for the analysis of physiologically relevant mutations in GPCRs associated with diseases, for example, Rho mutations that are associated with retinal degenerative processes.

Acknowledgments We thank Dr. Paul Hargrave and Dr. Clay Smith for providing us with an anti-rhodopsin antibody. This work has been supported by grants SAF2005-08148-C04-02 and Acciones Integradas Hispano-Alemanas (HA2006-0130) from the Spanish Ministry of Science (to PG). Support was also from a grant of the EWE Stiftung (to KWK) and from the Deutscher Akademischer Austauschdienst DAAD within the program Acciones Integradas Hispano-Alemanas (to KWK). MA is the recipient of a predoctoral FPI fellowship from the Spanish Ministry of Science and DT is the recipient of a predoctoral fellowship from Universitat Politècnica de Catalunya (UPC).

References

1. Palczewski K, Kumasaka T, Hori T, Behnke CA, Motoshima H, Fox BA, Le Trong I, Teller DC, Okada T, Stenkamp RE, Yamamoto M, Miyano M (2000) Crystal structure of rhodopsin: A G protein-coupled receptor. Science 289:739–745
2. Murakami M, Kouyama T (2008) Crystal structure of squid rhodopsin. Nature 453:363–367
3. Shimamura T, Hiraki K, Takahashi N, Hori T, Ago H, Masuda K, Takio K, Ishiguro M, Miyano M (2008) Crystal structure of squid rhodopsin with intracellularly extended cytoplasmic region. J Biol Chem 283:17753–17756
4. Schertler GF (2005) Structure of rhodopsin and the metarhodopsin I photointermediate. Curr Opin Struct Biol 15:408–415
5. Salom D, Lodowski DT, Stenkamp RE, Le Trong I, Golczak M, Jastrzebska B, Harris T, Ballesteros JA, Palczewski K (2006) Crystal structure of a photoactivated deprotonated intermediate of rhodopsin. Proc Natl Acad Sci USA 103:16123–16128
6. Park JH, Scheerer P, Hofmann KP, Choe HW, Ernst OP (2008) Crystal structure of the ligand-free G-protein-coupled receptor opsin. Nature 454:183–187
7. Cherezov V, Rosenbaum DM, Hanson MA, Rasmussen SG, Thian FS, Kobilka TS, Choi HJ, Kuhn P, Weis WI, Kobilka BK, Stevens RC (2007) High-resolution crystal structure of an engineered human beta2-adrenergic G protein-coupled receptor. Science 318:1258–1265
8. Koch K-W (2000) Identification and characterization of calmodulin binding sites in cGMP-gated channel using surface plasmon resonance spectroscopy. Methods Enzymol 315:785–797
9. Schuck P (1997) Use of surface plasmon resonance to probe the equilibrium and dynamic aspects of interactions between biological macromolecules. Annu Rev Biophys Biomol Struct 26:541–566
10. Alves ID, Salamon Z, Varga E, Yamamura HI, Tollin G, Hruby VJ (2003) Direct observation of G-protein binding to the human delta-opioid receptor using plasmon-waveguide resonance spectroscopy. J Biol Chem 278:48890–48897
11. Stenlund P, Babcock GJ, Sodroski J, Myszka DG (2003) Capture and reconstitution of G protein-coupled receptors on a biosensor surface. Anal Biochem 316:243–250
12. Kasheverov IE, Zhmak MN, Fish A, Rucktooa P, Khruschov AY, Osipov AV, Ziganshin RH, D'Hoedt D, Bertrand D, Sixma TK, Smit AB, Tsetlin VI (2009) Interaction of alpha-conotoxin ImII and its analogs with nicotinic receptors and acetylcholine-binding proteins: additional binding sites on Torpedo receptor. J Neurochem 111:934–944
13. Huang M, Lai WP, Wong MS, Yang M (2001) Effect of receptor phosphorylation on the binding between IRS-1 and IGF-1R as revealed by surface plasmon resonance biosensor. FEBS Lett 505:31–36
14. Vidic J, Pla-Roca M, Grosclaude J, Persuy MA, Monnerie R, Caballero D, Errachid A, Hou Y, Jaffrezic-Renault N, Salesse R, Pajot-Augy E, Samitier J (2007) Gold surface functionalization and patterning for specific immobilization of olfactory receptors carried by nanosomes. Anal Chem 79:3280–3290
15. Vidic JM, Grosclaude J, Persuy MA, Aioun J, Salesse R, Pajot-Augy E (2006) Quantitative assessment of olfactory receptors activity in immobilized nanosomes: a novel concept for bioelectronic nose. Lab Chip 6:1026–1032
16. Sen S, Jaakola VP, Pirila P, Finel M, Goldman A (2005) Functional studies with membrane-bound and detergent-solubilized alpha2-adrenergic receptors expressed in Sf9 cells. Biochim Biophys Acta 1712:62–70
17. Heyse S, Ernst OP, Dienes Z, Hofmann KP, Vogel H (1998) Incorporation of rhodopsin in laterally structured supported membranes: observation of transducin activation with spatially and time-resolved surface plasmon resonance. Biochemistry 37:507–522
18. Salamon Z, Wang Y, Brown MF, Macleod HA, Tollin G (1994) Conformational changes in rhodopsin probed by surface plasmon resonance spectroscopy. Biochemistry 33:13706–13711
19. Bieri C, Ernst OP, Heyse S, Hofmann KP, Vogel H (1999) Micropatterned immobilization of a G protein-coupled receptor and direct detection of G protein activation. Nat Biotechnol 17:1105–1108
20. Clark WA, Jian X, Chen L, Northup JK (2001) Independent and synergistic interaction of retinal G-protein subunits with bovine rhodopsin measured by surface plasmon resonance. Biochem J 358:389–397
21. Komolov KE, Senin II, Philippov PP, Koch KW (2006) Surface plasmon resonance study of g protein/receptor coupling in a lipid bilayer-free system. Anal Chem 78:1228–1234
22. Jastrzebska B, Maeda T, Zhu L, Fotiadis D, Filipek S, Engel A, Stenkamp RE, Palczewski K (2004) Functional characterization of rhodopsin monomers and dimers in detergents. J Biol Chem 279:54663–54675
23. Koch K-W, Lambrecht HG, Haberecht M, Redburn D, Schmidt HH (1994) Functional coupling of a Ca2+/calmodulin-dependent nitric oxide synthase and a soluble guanylyl cyclase in vertebrate photoreceptor cells. EMBO J 13:3312–3320
24. Kuhn H (1981) Interactions of rod cell-proteins with the disk membrane—influence of light, ionic-strength, and nucleotides. Curr Top Memb Transp 15:171–201

25. Bornancin F, Pfister C, Chabre M (1989) The transitory complex between photoexcited rhodopsin and transducin. Reciprocal interaction between the retinal site in rhodopsin and the nucleotide site in transducin. Eur J Biochem 184:687–698
26. Oprian DD, Molday RS, Kaufman RJ, Khorana HG (1987) Expression of a synthetic bovine rhodopsin gene in monkey kidney cells. Proc Natl Acad Sci USA 84:8874–8878
27. Liu X, Garriga P, Khorana HG (1996) Structure and function in rhodopsin: correct folding and misfolding in two point mutants in the intradiscal domain of rhodopsin identified in retinitis pigmentosa. Proc Natl Acad Sci USA 93:4554–4559
28. Lange C, Koch KW (1997) Calcium-dependent binding of recoverin to membranes monitored by surface plasmon resonance spectroscopy in real time. Biochemistry 36:12019–12026
29. Alves ID, Salgado GFJ, Salamon Z, Brown MF, Tollin G (2005) Phosphatidylethanolamine enhances rhodopsin photoactivation and transducin binding in a solid supported lipid bilayer as determined using plsmon-waveguide resonance spectrscopy. Biophys J 88:198–210
30. Getmanova E, Patel AB, Klein-Seetharaman J, Loewen MC, Reeves PJ, Friedman N, Sheves M, Smith SO, Khorana HG (2004) NMR spectroscopy of phosphorylated wild-type rhodopsin: mobility of the phosphorylated C-terminus of rhodopsin in the dark and upon light activation. Biochemistry 43:1126–1133
31. Langen R, Cai K, Altenbach C, Khorana HG, Hubbell WL (1999) Structural features of the C-terminal domain of bovine rhodopsin: a site-directed spin-labeling study. Biochemistry 38:7918–7924
32. De Grip WJ (1982) Thermal stability of rhodopsin and opsin in some novel detergents. Methods Enzymol 81:256–265
33. Aveldano MI (1995) Phospholipid solubilization during detergent extraction of rhodopsin from photoreceptor disk membranes. Arch Biochem Biophys 324:331–343
34. Garriga P, Liu X, Khorana HG (1996) Structure and function in rhodopsin: correct folding and misfolding in point mutants at and in proximity to the site of the retinitis pigmentosa mutation Leu-125→Arg in the transmembrane helix C. Proc Natl Acad Sci USA 93:4560–4564
35. Wong JP, Reboul E, Molday RS, Kast J (2009) A carboxy-terminal affinity tag for the purification and mass spectrometric characterization of integral membrane proteins. J Proteome Res 8:2388–2396